Honors Draft

Raven McKnight

2/9/2020

Abstract

abstract

1 Introduction

Public transit ridership has been in decline around the country for years, but particularly since the mid 2010s (). Following a spike in ridership related to the 2008 housing market crash, ridership has been steadily trending downwards in most metropolitan areas (). Bus ridership is particularly affected compared to more "desirable" light rail and commuter rail. Transit agencies are naturally interested in understanding the specific causes of these declines, as well as more generally being able to predict transit demand throughout space and time.

Transit ridership, or demand, is often forecasted using models from the policy and planning world, such as the classic four-step model. Four-step transportation demand models consist of simulating trips and their spatial distribution before assigning them modes (ie bus versus car versus bicycle) and routes. Other models, called activity-based models predict transportation demand based on when and where riders are likely to conduct various tasks (commuting, shopping, recreation, etc). Others still are based largely on land-use characteristics under the general premise that different types of development (or lack thereof) are more or less likely to draw riders.

It is somewhat rare to see more traditional statistical models applied to transit ridership. In the context of predicting future ridership, the above methods are often sufficient. Additionally, they are the industry standard and allow for the integration of expert planning knowledge. However, in the context of understanding *past* ridership, we can apply more explanatory methods. Specifically, we can use hierarchical spatial Bayesian models to incorporate many covariates in addition to the spatial structure that necessarily underpins transit ridership (ie, boardings can only occur at existing bus stops).

Hierarchical spatial models allow us to understand the patterns of ridership within a city with great granularity. Some existing literature explores the decline of transit ridership *between* cities (). Few studies have been conducted on the various patterns of ridership *within* a single metropolitan area. Additionally, few studies incorporate many demographic predictors. Naturally, we cannot collect demographic information for every rider of a transit system. Instead, we can use demographic predictors associated with spatial units such as census block groups to explore the question of *who* rides – or, at the very least, *where* do they ride.

2 Background

2.1 Metro Transit

Metro Transit is the primary transit provider in the Minneapolis-Saint Paul metropolitan area. The agency operates one commuter rail line (Northstar), two light rail lines (Blue Line and Green Line), and over 100

bus routes. Since the 2014 opening of the Green Line, rail ridership has increased each year (). Bus ridership, however, has been in decline. According to the Metro Transit Riders' Almanac blog, much of the decline is bus ridership can be attributed to the busiest urban local routes as well as situational factors, such as lower-than-average gas prices and a system-wide fare increase in 2017.

The agency is naturally interested in understanding with more detail the reasons for and nature of these declines.

Conducted in tandem with Metro Transit's Network Next bus system redesign, this study aims to further Metro Transit's understanding of their bus network. Specifically, we aim to describe the existing pattern of transit ridership via demographic predictors and spatial patterns. Future work will incorporate temporal trends to better understand declining ridership.

2.2 Transit Market Areas

Metro is interested in predicting transit demand across the region in order to guide route planning and service provision. Currently, Metro Transit uses a set of 5 Transit Market Areas to estimate spatial demand. The Transit Market Areas are written into the official Transportation Planning Policy (TPP) and are calculated using a simple linear regression. Following the notation of the TPP, the formula for determine Transit Market Areas is expressed

$$\begin{aligned}\text{Transit Market Index } &= 0.64 * \text{Population Density} + 0.20 * \text{Employment Density} + \\ &\quad 0.23 * \text{Intersection Density} + 0.11 * \text{Automobile Availability}\end{aligned}$$

where each predictor is logged and scaled by developed land acreage per census block group. Here, automobile availability refers to the number of adults over age 16 less the total number of automobiles available in a block group (scaled by developed land acreage). There is an additional indicator variable, omitted in this notation, for the census block group containing the MSP International Airport. For more documentation of the official Transit Market Areas, refer to the TPPs Appendix G.

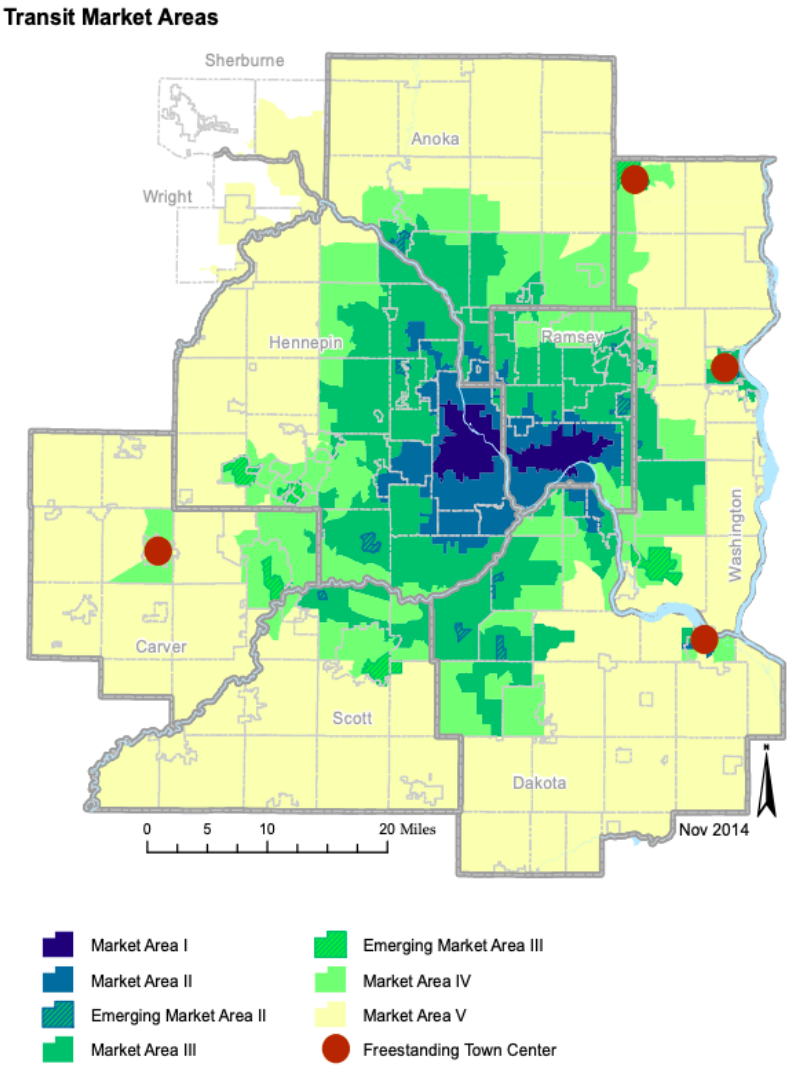

Figure 1: Metro Transit's Transit Market Areas from Metropolitan Council's Transportation Planning Policy, Appendix G.

Census block groups are split into 5 market areas based on the Transit Market Index described above, where the highest market area (Market Area 1) is expected to support high-frequency, all-day service and the lowest market area (Market Area 5) is expected to support peak commuter express service and park-and-rides, if that.

The Transit Market Index values are geographically smoothed to create more-or-less concentric Transit Market Areas. The linear regression is an intuitive way to think about transit ridership across space. The four predictors used are common-sense indicators of transit ridership: high population and employment density are characteristic of trip origins and destinations, automobile availability is reasonably assumed to be related to transit ridership, and intersection density is a proxy for the "walkability" of an area. However, the existing Transit Market Area model may be over-simplifying the complex question of transit ridership.

3 Data

3.1 Metro Transit Data

This analysis relies on several Metro Transit provided data sets. The two primary sources are automatically reported by in-service vehicles, yielding billions of rows of observations.

Automatic Passenger Count (APC) data is reported every time a bus opens its doors. Two beams of light detect movement through the doors of the bus and counts the number of passengers getting on and off at each bus stop. Naturally, this data source is flawed: sometimes, vehicles fail to report data, and the sensors can be easily tricked. Someone getting off the bus pulling a suitcase behind them, for example, would likely be counted as two passengers exiting. However, APC is the most granular ridership data available, giving us the most control over our spatial aggregations of ridership. This is the primary data source used in this analysis.

Automatic Vehicle Location (AVL) data is similarly reported by in-service vehicles (approximately) every 8 seconds. The vehicle reports in GPS location continuously while in service. We use AVL data to adjust for missing APC data.

Metro Transit's Schedule as *planned*, rather than as *run*, is also used to correct missing APC data.

This analysis began by pulling all APC, AVL, and schedule data from 2015-2018. The initial data pull consisted of approximately 496 *billion* rows of data. The analysis presented here focuses on 2017 data. Figure *____* shows the average weekday boardings by census block group in 2017.

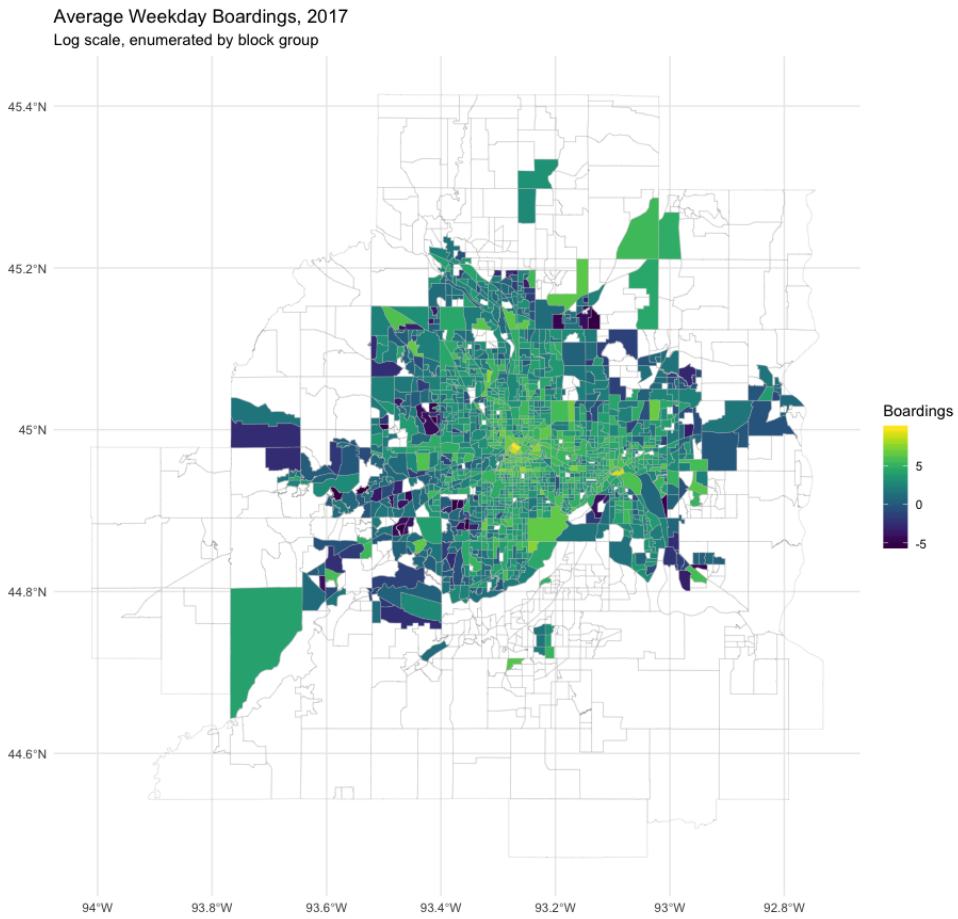

Figure 2: Average weekday boardings by census block group, the response variable for this analysis.

3.1.1 Data Interpolation

In theory, we have APC data for each run bus trip in 2017. However, we know that, for a variety of reasons, this is untrue. The automatic data reporting technology on Metro Transit buses is flawed and can fail to report data unpredictably. Additionally, the trips missing data may not be random: all buses of one "series", for example, may fail to report at once. This could lead to the APC dataset underestimating boardings on a particular set of routes or locations.T therefore, we use the three data sets described above to create a more complete augmented APC data set.

The algorithm used to interpolate data works essentially as follows:

1. Compares scheduled trips to trips we have APC data for. If a trip was scheduled but has no APC records, we consider that trip missing.
2. For missing trips, check AVL data. If there are no AVL records, we consider the trip cut (ie, we assume the trip was not run).
3. For missing trips with AVL data, we estimate boardings for that trip by taking the average number of boardings for trips of that nature (trips on the same route, day of week, season, location, etc).

3.1.2 Data Aggregation

For the models presented in this study, we aggregate boardings at individual bus stops to the census block group. This is in large part to match the granularity of the American Community Survey covariates we are interested in using. Future work could explore using areal covariates to model ridership at specific points (ie, bus stops).

Additionally, we aggregate boardings counts to average weekday boardings. This a) greatly reduces the number of rows of data in play, and therefore shortens computation time significantly, and b) allows us to build a spatial model without simultaneously incorporating temporal trends. The data interpolation described above will be more impactful in future studies incorporating temporal trends.

3.2 Other data sources

All other data sources used in this study are from outside sources. Census Block Groups are used as the areal unit of analysis. Covariates of interest are primarily from the 2017 American Community Survey (ACS) 5-Year Estimates. Additional variables related to employment are sourced from the Longitudinal Origin-Destination Employment Statistics (LODES) dataset. A full list of covariates used in this study is below.

Parameter	Meaning
beta[1]	median household income
beta[2]	percent residents identified as white alone
beta[3]	area of 10 minute walk isochrone from population-weighted block group centroid
beta[4]	percent residents with a high school diploma
beta[5]	percent residents with a bachelor's degree
beta[6]	percent of residents who rent their residence
beta[7]	percent of residents without a vehicle
beta[8]	percent of residents who speak only English
beta[9]	percent of residents identified as foreign
beta[10]	employment density
beta[11]	percent of jobs in block group for white employees
beta[12]	percent of jobs in block group for male employees
beta[13]	percent of jobs in block group for employees with no college degree
beta[14]	percent of jobs in block group for employees who make less than $40,000
beta[15]	percent of jobs in block group for employees under age 30
beta[16]	median age
beta[17]	percent residents who use transit to commute to work
beta[18]	population density

Table 1: List of covariates

Note that `beta[3]` is a measure of walkability. A 10-minute walk isochrone, generated using OpenTripPlanner, shows the area a person on foot can cover in 10 minutes on the existing street network. In theory, we expect more walkable areas, such as the downtown Saint Paul and Minneapolis, to have larger walk-isochrones. Unfortunately, the metric can be fooled by rural areas where you can walk uninterrupted down a single roadway, for example. An improved "walkability" metric could improve models of transit ridership.

Nearly all studies of transit ridership incorporate some measure of employment density. Few incorporate anything more granular than number of jobs per acre or square mile. This study incorporates more detailed employment characteristics from LODES in an attempt to better isolate groups of riders in addition to areas of high ridership.

All covariates in the table above are standardized to have mean 0 and standard deviation 1. Intuitively, we expect many of the covariates to be correlated. Therefore, we will utilize variable selection to determine which covariates to keep in our analysis.

4 Models

4.1 Stan

All of the models discussed above can be fit using the programming language Stan. Stan is a probabilistic language which uses Hamiltonian Monte Carlo (HMC) and a specialized No U-Turn Sampler (NUTS) to compute joint log probability densities. The specifics of Stan are beyond the scope of this paper. However, a few of its particular diagnostics are helpful in understanding the differences between the model fits below.

- $\hat{R}$ or `Rhat` indicates how well the Markov chains have mixed by comparing between- and within-chain estimates. At convergence, $\hat{R} = 1$. When $\hat{R} > 1$, the Markov chains have not mixed well and the model likely needs to be run for more iterations.

- `n_eff` is the estimated Effective Sample Size (ESS). ESS is the number of independent samples our sample is equivalent to. In other words, if `n_eff` = 1,000, we expect to gain the same amount of information from our sample as we would from 1,000 independent samples. In a "perfect" scenario, `n_eff` should equal the actual number of samples. When `n_eff` is significantly below the actual number of samples, there may be a problem with the model and posterior estimates may be biased.
- **Divergent transitions** occur when the simulated Hamiltonian departs from the actual Hamiltonian trajectory. In general, if stan gives any divergent transition warnings, we should consider the posterior estimates unreliable.

- `max_treedepth` is a parameter we set when fitting a model in Stan. Treedepth refers to the number of steps the sampler has to take at each iteration. The default is 10. For extremely "curved" or complex posteriors, the treedepth may be much higher. When `max_treedepth` is exceeded, the sampler quits prematurely. Therefore, if we have *many* iterations exceeding `max_treedepth`, posterior estimates may be unreliable. Additionally, setting high treedepth causes the sampler to perform much more slowly.
- `adapt_delta` is also a sampling parameter; it corresponds to the Mean Metropolis Acceptance Rate (see _____). The default is 0.8. Setting a higher `adapt_delta` slows computation time but *can* eliminate "false alarm" divergent transitions.

4.2 Poisson Regression

For each block group $i = 1, 2, 3, ..., 1495$ with any ridership, the "baseline" model is a simple Poisson regression. Poisson regressions are a type of generalized linear model with the natural log as its link function. For ridership Y_i and covariates $x_1, ..., x_k$ discussed above, the Poisson regression is written

$$\begin{aligned} Y_i &\sim \text{Poisson}(E_i \lambda_i) \\ \eta_i = log(\lambda_i) &= \beta_0 + \sum_{k=1}^{K} x_k^T \beta_k \\ \beta_0, \beta &\sim \text{Normal}(0, 1) \end{aligned}$$

where β_0 is the intercept and E_i is an offset term.

The offset E_i is often termed "exposure" in applications such as disease risk modeling where the offset may be the number of observed cases in a previous year, for example. More technically, the offset term scales

the Poisson output to be a rate rather than a count. This is appropriate when observations i have different potentials for response Y. For example, a county with higher population will naturally have a higher count of patients with asthma than a county with a smaller population. Mathematically, the offset is a covariate with parameter set equal to 1. Recall, the Poisson regression assumes we can model the mean of response Y, $\bar{Y}$ with a combination of linear predictors:

$$log(\bar{Y}) = \beta_0 + \sum_{k=1}^{K} x_k^T \beta_k$$

Therefore, if we wish to model the rate Y/E, the equation is rewritten

$$log(\bar{Y}/E) = \beta_0^{'} + \sum_{k=1}^{K} x_k^T \beta_k^{'}$$

$$log(\bar{Y}) = log(E) + \beta_0^{'} + \sum_{k=1}^{K} x_k^T \beta_k^{'}$$

In this study, we define E_i to equal the number of times a bus stops in block group i. This allows us to control for block groups with more or less supply.

In the basic Poisson regression, we often give β_0 and β vague priors such as Normal$(0, 1)$. The exposure term E_i comes from the data and does not receive a prior.

4.2.1 Model 1

We will call this baseline Poisson regression Model 1. Model 1 uses all 18 covariates with simple Normal(0, 1) priors and no overdispersion parameters. The Stan program used to fit Model 1, as well as the other four models, can be found in the appendix. Low autocorrelation between iterations allows Model 1 to fit quickly and efficiently. The Stan output for β_0 and β is below.

Parameter	Rhat	n_eff	mean	sd	2.5%	97.5%
beta_0	1.000	19365	-1.376	0.005	-1.385	-1.366
beta[1]	1.000	18085	0.006	0.007	-0.007	0.019
beta[2]	1.000	19330	0.063	0.005	0.054	0.072
beta[3]	1.000	18752	-0.027	0.004	-0.035	-0.019
beta[4]	1.000	18026	-0.029	0.004	-0.038	-0.021
beta[5]	1.000	18380	-0.013	0.005	-0.022	-0.004
beta[6]	1.000	15809	0.241	0.005	0.231	0.251
beta[7]	1.000	18930	0.014	0.003	0.007	0.020
beta[8]	1.000	17331	-0.003	0.005	-0.012	0.006
beta[9]	1.000	19360	0.074	0.004	0.067	0.082
beta[10]	1.000	21329	0.066	0.001	0.065	0.068
beta[11]	1.000	20224	-0.121	0.004	-0.128	-0.114
beta[12]	1.000	22539	-0.069	0.004	-0.076	-0.061
beta[13]	1.000	18372	-0.011	0.005	-0.021	-0.001
beta[14]	1.000	15602	-0.026	0.005	-0.035	-0.017
beta[15]	1.000	15480	0.113	0.005	0.104	0.122
beta[16]	1.000	19904	-0.085	0.004	-0.093	-0.078
beta[17]	1.000	21169	0.047	0.003	0.042	0.053
beta[18]	1.000	22032	-0.025	0.003	-0.031	-0.020

Table 2: Stan output for Model 1

Model 1 produces coefficient estimates with tight confidence intervals; few of the β_k 95% intervals cross zero.

Notably, β_6, or percent of residents who rent their residence, has the largest magnitude of any coefficient. This finding confirms Metro Transit's belief that "impermanence" is a good predictor of transit ridership. Broadly, "impermanence" or "instability" related with being a recent immigrant, a single parent, or even a student is expected to have a strong positive correlation with ridership. It is a novel finding within the agency that percent of residents who rent their home is a "stronger" predictor of ridership than more intuitive predictors such as median household income (in this model, the coverage interval for median household income ($\beta[1]$) crosses zero!).

Unfortunately, our 10-minute walk isochrone approximation of walkability β_2 is shown to have a negative correlation with average daily boardings. This suggests that the metric for walkability needs to be improved because we know inherently that walkability should increase ridership.

In addition to our flawed walkability metric, parameters $\beta_4, \beta_5, \beta_8, \beta_{11}, \beta_{12}, \beta_{13}, \beta_{14}, \beta_{16}$, and$\beta_{18}$ are negatively associated with daily boardings. The fact that $\beta_1 8$, population density, is negatively correlated with ridership suggests that this model is flawed: population density is widely accepted as one of the most important predictors for transit ridership.

Based on initial diagnostics and precise parameter estimates, Model 1 appears to be a "good" fit. However, posterior predictive checking reveals shortcomings in Model 1's fit. Figure ___ shows the observed distribution of Y in dark blue overlaid with 100 simulated observations of Y produced by Model 1. In a well-fitting model, the simulated Y should closely follow the observed distribution.

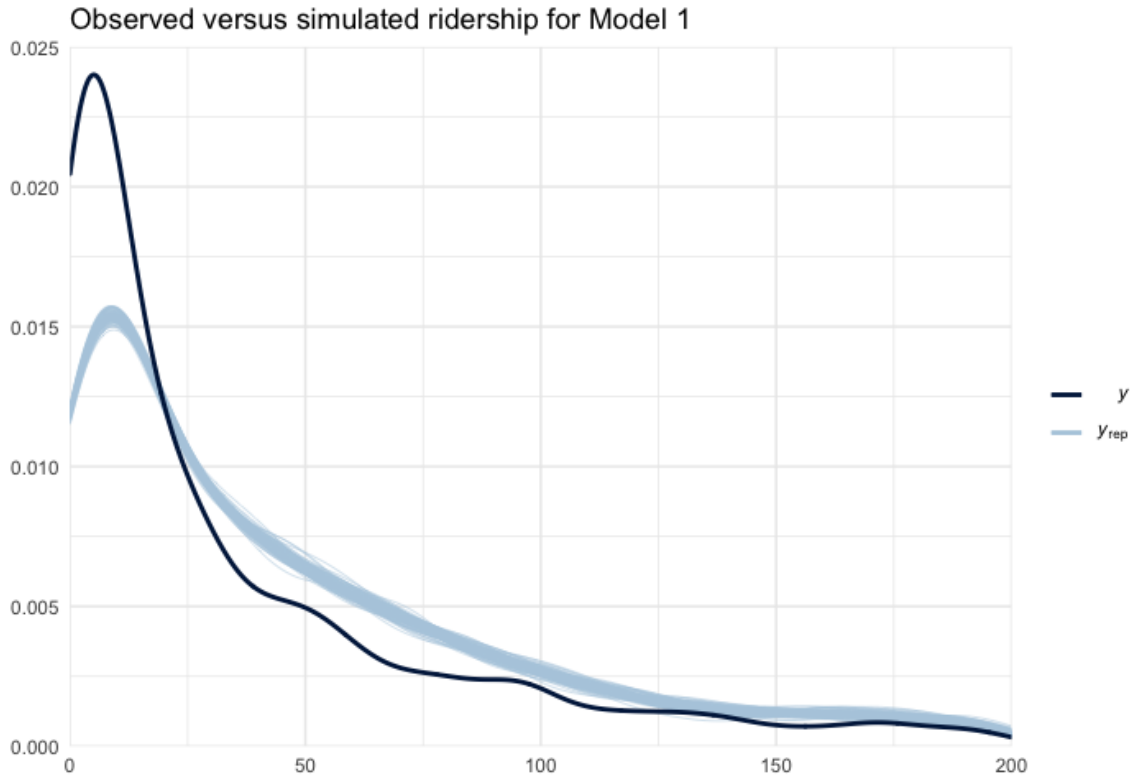

Figure 3: Posterior predictive check for Model 1.

Model 1 clearly underestimates the number of block groups with low ridership. This is due in large part to extra-Poisson variance present in Metro Transit's ridership data.

Figure ___ maps observed versus simulated ridership. Visually, we can detect areas which are markedly different between the actual versus estimated boardings: the model tends to overestimate ridership in "mid-

dle ridership" areas (ie, block groups that are in neither the high-activity urban core nor the low-density rural/suburban outskirts of the metro area).

4.3 Overdispersed Poisson Regression

The most obvious assumption made in a Poisson regression is that response variable Y follows a Poisson distribution. In addition to requiring integer counts, this assumption requires that $\text{Var}(Y) = \text{E}(Y)$. This is often not true in practice. In the case of the Metro Transit ridership data, $\text{Var}(Y) >> \text{E}(Y)$. In this case, we call the unexpectedly large variance "overdispersion" or "extra-Poisson variance."

Data with this feature can be difficult to model directly with a Poisson regression. One option is to use a generalization of the Poisson distribution, such as a Negative-Binomial distribution, as the observation model. For the Metro Transit application, we instead modify the latent function to include a separate term to account for overdispersion. As such, the Poisson regression above can be rewritten to include

$$\begin{aligned} \eta_i = log(\lambda_i) &= \beta_0 + \sum_{k=1}^{K} x_k^T \beta_k + \theta\sigma \\ \theta &\sim \text{Normal}(0, 1) \\ \sigma &\sim \text{Normal}(0, 5) \end{aligned}$$

where θ is a set of heterogeneous random effects. In practice, θ is scaled by its variance parameter σ to allow easier fitting in Stan. The addition of this set of random effects improves fits on data with overdispersion. With sufficiently vague priors, θ and σ can account for most or all of the overdispersion not accounted for by $\beta_0 + \sum_{k=1}^{K} x_k^T \beta_k$.

4.3.1 Model 2

Model 2 builds upon Model 1 by incorporating the set of random effects described above. Model 2 is *significantly* more computationally expensive to fit than Model 1. This is due to relatively large autocorrelation between each iteration, visible in the trace plots below (Figure ____). This autocorrelation made it necessary to run Model 2 on four chains for 20,000 iterations each. Despite this, `n_eff` is significantly lower for Model 2 than Model 1. Model 2 also experienced 2 transitions exceeding maximum treedepth: not a problem in terms of model fit, but a signal that the posterior is more challenging to fit. Reparameterization could likely reduce autocorrelation between iterations.

The parameter estimates for β_0 and β for Model 2 are below. Notably, the direction and magnitude of the coefficient estimates are similar to those produced by Model 1. Specifically, influential parameters such as β_6 remain influential in this setting. However, the coverage intervals for all β_k are much wider. Based on "test runs" of Model 2, we expect increasing the number of iterations to decrease the width of these coverage intervals (we observe that the width of the coverage interval is proportional to the number of iterations in this setting).

Parameter	Rhat	n_eff	mean	sd	2.5%	97.5%
beta_0	1.0	1354	-1.9	0.0	-2.0	-1.8
sigma	1.0	1800	1.0	0.0	0.9	1.0
beta[1]	1.0	1546	-0.1	0.0	-0.2	-0.0
beta[2]	1.0	1095	0.0	0.1	-0.1	0.1
beta[3]	1.0	1322	0.0	0.0	-0.0	0.1
beta[4]	1.0	1208	-0.0	0.0	-0.1	0.0
beta[5]	1.0	1282	-0.0	0.0	-0.1	0.1
beta[6]	1.0	988	0.1	0.0	0.1	0.2
beta[7]	1.0	1019	0.1	0.0	-0.0	0.1
beta[8]	1.0	1178	0.0	0.0	-0.0	0.1
beta[9]	1.0	1125	0.0	0.0	-0.1	0.1
beta[10]	1.0	1796	0.1	0.0	0.1	0.2
beta[11]	1.0	1152	-0.1	0.0	-0.1	-0.0
beta[12]	1.0	1629	0.0	0.0	-0.0	0.1
beta[13]	1.0	2101	-0.0	0.0	-0.1	0.0
beta[14]	1.0	1415	-0.1	0.0	-0.1	-0.0
beta[15]	1.0	1581	0.1	0.0	0.0	0.2
beta[16]	1.0	1160	-0.1	0.0	-0.2	-0.0
beta[17]	1.0	997	0.1	0.0	0.0	0.2
beta[18]	1.0	1589	-0.0	0.0	-0.1	0.0

Table 3: Stan output for Model 2

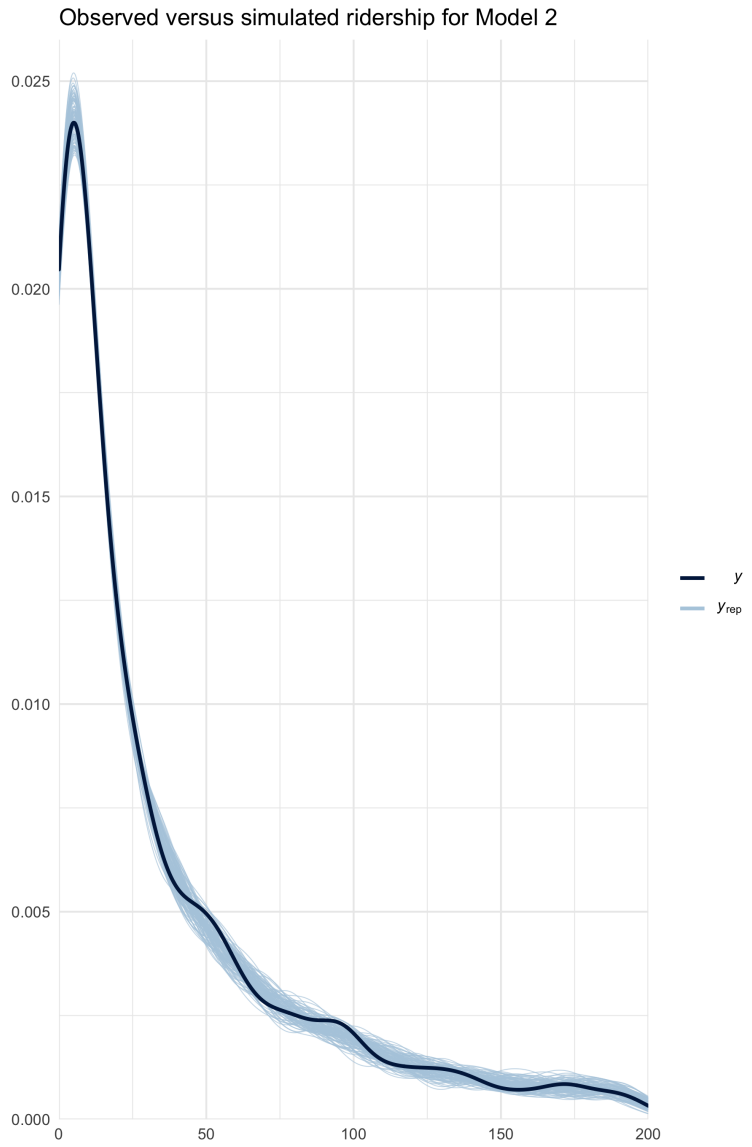

Figure 4: Posterior predictive check for Model 2.

Because we gave θ and σ vague priors, we can see a *much* better fit in the posterior predictive checks for Model 2. As above, Figure ___ maps the observed ridership by block group versus the ridership simulated by Model 2.

One *could* stop analysis here. However, the addition of $\theta\sigma$ only improves the *fit* of the model, not our understanding of the data. Therefore, for this study, we will decompose $\theta\sigma$ into spatial and non-spatial random effects. First, however, we will implement a Bayesian variable selection process to determine which, if any, of our covariates x_k should be removed from the analysis.

4.4 Horseshoe Priors and Variable Selection

In the baseline model, we give coefficients $\beta_1, ..., \beta_k$ simple normal priors. With a large set of possible covariates, however, we may reasonably expect some of the β_k coefficients to be equal to zero – in other words, that some of the parameters x_k have no effect on response Y. In frequentist applications, we might

use a method such as the LASSO (Least Absolute Shrinkage and Selection Operator) to identify relevant variables. There are several Bayesian alternatives for variable selection with generally consist of applying particular priors to β.

4.4.1 Spike and Slab - needs graphics

In the Bayesian setting, there are two primary methods for variable selection. The first is called the "spike-and-slab" prior (Mitchell and Beauchamp, 1988; George and McCulloch, 1999) and has often been considered the "gold standard" for sparse Bayesian regression, or variable selection (Piironen and Vehtari, 2017). This prior is often expressed as

$$\begin{aligned}\beta_j|\lambda_j, c, \epsilon &\sim \lambda_j \text{Normal}(0, c^2) + (1-\lambda_j)\text{Normal}(0, \epsilon^2) \\ \lambda_j &\sim \text{Bernoulli}(\pi)\end{aligned}$$

for $j = 1, 2, ..., J$ where $\lambda_j \in 0, 1$ indicates whether β_j is from the "spike" (ie, near zero) or the "slab" (ie, nonzero). The "spike" is the area where most of the prior density for β is centered (generally around 0) while the "slab" refers to the low-density extent of the prior. The spike-and-slab prior encourages all β_j towards zero; only β_j sufficiently far from 0 will be estimated to be from the slab.

The primary challenge with the spike-and-slab (and other Bayesian shrinkage methods) is the Selection of priors. Priors must be set for the width of the slab c and the prior inclusion probability π. Here, π reflects our prior understanding of the sparsity of β. In practice, we rarely have strong prior knowledge of the number of predictors we expect to be distinguishable from zero. This can make the implementation of sparse regression more challenging than, say, the frequentist LASSO.

4.4.2 Horseshoe - needs graphics

The second method for Bayesian sparse regression is to give β some continuous *sparsity inducing prior*. **Van Erp et al (2019)** provide an introduction to many such continuous priors. Ridge regression and the Bayesian LASSO are two of the most approachable priors, but all sparsity inducing priors utilize the same logic as the spike-and-slab: give β a prior with *most* of its mass near 0, to shrink irrelevant coefficients, and the rest of its mass "far" from 0. Identifying "far" depends more or less on the specific data and model in question.

The horseshoe prior, proposed by **Carvalho et al, 2010** is a popular choice in Bayesian literature, in part because it is similar to the "gold standard" spike-and-slab. Following the notation of **Vehtari & Piironen**, the horseshoe prior can be expressed

$$\begin{aligned}\beta_k \mid \lambda_k, \tau &\sim \text{Normal}(0, \tau^2\lambda_k^2) \\ \lambda_k &\sim \text{Half-Cauchy}(0, 1)\end{aligned}$$

for $k = 1, 2, ..., K$. The horseshoe prior is so-named because for fixed values $\tau = \lambda_k = 1$, the prior resembles a Beta(1/2, 1/2) distribution, or a horseshoe.

The horseshoe is often favored because it is a global-local shrinkage prior. This means that τ shrinks *all* parameters towards 0 while the local parameter λ_k and the heavy Cauchy tails allow larger coefficients to remain unshrunk. While this is precisely the goal of a sparsity inducing prior, the horseshoe prior can fail to regularize large coefficients *at all*, which can be a problem when parameters are weakly identified by data. With no regularization applied to the largest coefficients, there is a risk of overfitting. Additionally, there is no consensus in the literature for assigning priors to *tau*. Piironen and Vehtari (2017) introduced the *regularized horseshoe* to address both of these shortcomings of the horseshoe.

4.4.3 Regularized Horseshoe - needs graphics

The regularized horseshoe builds upon the horseshoe prior such that

$$\begin{aligned}
\beta_k \mid \lambda_j, \tau, c &\sim \text{Normal}(0, \tau^2 \tilde{\lambda}_k^2) \\
\tilde{\lambda}_k^2 &= \frac{c^2 \lambda_k^2}{c^2 + \tau^2 \lambda_k^2} \\
\lambda_k &\sim \text{Half-Cauchy}(0, 1) \\
c &\sim \text{Inverse-Gamma}(a, b)
\end{aligned}$$

where $c > 0$ helps to regularize β_k far from zero. When c approaches infinity, the regularized horseshoe becomes the standard horseshoe. Additionally, c in the regularized horseshoe corresponds to the slab width in the spike-and-slab prior.

As with the spike-and-slab, the selection of priors is a challenge with the regularized horseshoe. Piironen and Vehtari (2017) provide a set of recommendations for setting priors which we follow in this study. In practice, we tune the priors for λ_k, c, and τ using simulated data with features similar to our observed data (ie, parameters with coefficients of similar magnitude).

4.4.4 Model 3

For this study, we implement the regularized horseshoe using code modified from Piironen & Vehtari. We set priors following Piironen & Vehtari's recommendations. The priors assumed a priori that approximately half of the 18 covariates described in section ___ are relevant. This choice was made based on the assumption that many of the covariates are correlated and therefore may be redundant.

Like Model 2, this model requires 20,000 iterations for each of four chains to converge and produce suitably large Effective Sample Sizes. This model is more complex and slower still than Model 2 to fit. Both the overdispersion parameter as currently programmed in Stan and the sparsity inducing priors contribute to overall computation time.

Notably, Model 3 experienced one divergent transition after warmup. However, the model was fitted several times with no divergent transitions. A "false alarm" divergent transition can occur when the cutoff for determining a divergent transition is too low; this can be true in the case of particularly complex posteriors. Because only 1 out of 20,000 iterations produced a divergent transition, we can proceed with caution using Model 3. Additionally, the parameter estimates provided by Model 3 closely match those from Models 1 and 2, suggesting that the single divergent transition did not have an adverse effect on the posterior estimates.

The posterior predictive checks for Model 3 match Model 2 almost perfectly - this is to be expected. The addition of horseshoe priors on β_k does not attempt to improve model fit, but to determine which covariates are most "important".

We can see that Model 3 *did* shrink two β_k exactly to zero. Based on our priors, we expected more than two priors to be shrunk. The fact that more coefficients were not shrunk suggests that, despite being correlated, nearly all of the 18 selected covariates have some relevance. We expect horseshoe priors to be more helpful in modeling contexts with significantly more parameters and less confidence in their importance.

4.5 Adding Spatial Structure

When modeling data with a spatial component, we generally expect adjacent areas to be more similar than areas which are far apart. While this is a straightforward assumption, it can improve model fits in several ways. First, it can encode prior information about response Y not otherwise represented by covariates x (ie, that nearby observations are more similar than far-flung ones). Second, it can provide geographic smoothing when observations are sparse or noisy. This is often the case in small areas or when observing events which

can only occur at specific locations, such as air quality measured by sensors. In the case of the Metro Transit ridership data, this smoothing can help avoid overfitting areas such as the outliers in downtown Minneapolis and better represent block groups with no existing bus stops.

In the case of Metro Transit's ridership data, we expect encoding spatial structure to improve the model fit in several ways. First, we know that assigning transit ridership to census geography is inherently flawed. This is because census geographies, including block groups, are generally bounded by major roads (in addition to natural features such as lakes and political boundaries such as city limits). Naturally, bus stops tend to exist along those same major roadways.

need map to illustrate this section This bounding convention means that boardings are often assigned to different block groups depending on which direction the passenger is travelling. For example, consider the A-Line running along Snelling Avenue. Boarding at Snelling and Grand *northbound* puts you in block group _____ while boarding at the same intersection but *southbound* puts you in block group _____. Integrating spatial structure will help to smooth ridership across block group bounds. **will add a map here**

Additionally, we know intuitively that transit riders don't necessarily board in the block groups they live in. Particularly in dense areas, it's very likely for riders to board in a block group other than the block group they reside in. For example, I live in block group ___ but walk about 10 minutes to board the A-Line southbound at Snelling and Randolph in block group ___. Commuting patterns such as these can assign ridership to different block groups than we might expect. Geographic smoothing will allow neighboring block groups to share information, better representing these ridership patterns.

4.5.1 Conditional Autoregressive Priors

Conditional Autoregressive (CAR) priors are one of the most widespread Bayesian methods for modeling spatial autocorrelation. CAR models were introduced in Besag 1974 and remain perhaps the primary method for Bayesian areal data modeling. Note that CAR models are recommended for use as *priors* rather than as an observation model.

Areal data corresponds to finitely many discrete areal units, such as counties or census tracts. CAR priors are often used in the context of small-area count data. This sort of response variable tends to be noisy, particularly when the counted event is rare, the population of areal unit i is small, or the physical boundaries of areal units present challenges. CAR priors were designed in part to smooth such noisy counts. As such, they are often applied in epidemiological disease risk modeling in which disease occurrences may be rare.

Generally, CAR models rely on a binary neighborhood structure. Areal units i and j are considered neighbors if they share a boundary. For strictly rectangular lattice data, we often choose either a "Queens" or "Rooks" neighborhood structure. **insert graphics** For irregularly shaped areal data, such as our 1,495 census block groups, we generally default to a queen neighborhood structure wherein areal units sharing *any* points of contact are deemed neighbors.

For n regions, the neighborhood relationships are encoded in an $n \times n$ neighborhood matrix W. Matrix W is defined such that $w_{ij} = 1$ if if regions i and j are neighbors (denoted $i \sim j$) and 0 otherwise. This matrix is symmetric. Note that regions are not considered neighbors of themselves, ie the diagonal entries $w_{ii} = 0$.

The spatial interactions are modeled by a random variable ϕ. Here, ϕ is a vector $\phi = \phi_1, \phi_2, ..., \phi_n$. The distribution of each ϕ is determined by the sum of its neighbors' values such that

$$\phi_i \mid \phi_j, j \neq i \sim \text{Normal}(\sum_{i=1}^{N} w_{ij}\phi_j, \sigma^2)$$

The conditional distribution of each ϕ_i is helpful in building intuition about the functionality of the CAR prior. Basing the value of each ϕ_i off of its neighbors is how the CAR prior performs spatial smoothing.

Besag (1974) proved that the joint distribution of ϕ is a multivariate normal centered at 0 where its variance is given by a symmetric positive definite precision matrix Q. Matrix Q is simply the inverse of the covariance matrix $\sum$. This finding simplifies the above to

$$\phi \sim \text{Normal}(0, Q^{-1})$$

Precision matrix Q can be defined for multivariate normal ϕ using two other $n \times n$ matrices: the neighborhood matrix W and the diagonal matrix D in which d_{ii} indicates the number of neighbors region i has. All off-diagonal entries are 0. Using these matrices, Q is defined

$$Q = D(I - \alpha W)$$

where I is the identity matrix and $\alpha \in (0, 1)$ determines the amount of spatial autocorrelation present in Y. Parameter α is a key component of CAR models. At $\alpha = 0$, the model assumes spatial independence and at $\alpha = 1$, perfect spatial autocorrelation.

Following Morris et al, the log probability density of ϕ is proportional to

$$\frac{M}{2}\log(\det(Q)) - \frac{1}{2}\phi^T Q \phi$$

Calculating this value is computationally expensive. For models with 1,000 areal units, for example, calculating the determinant requires 1 billion operations (Morris et al, 2019). Given that the Metro Transit ridership data corresponds to 1,495 areal units, a strict CAR prior may be too computationally inefficient for our models.

4.5.2 Intrinsic Conditional Autoregressive

The Intrinsic Conditional Autoregressive (ICAR) prior is a slight simplification of a CAR prior. ICAR priors set $\alpha = 1$ which simplifies the definition of Q

$$Q = D - A$$

thereby setting $det(Q) = 0$. As a result, the first term in **equation ____** can be simplified to

$$-\frac{1}{2}\phi^T Q \phi$$

This reduces the computational expense of computing CAR models significantly. Notably, the ICAR prior is improper but yields proper posteriors (Morris et al, 2019).

The ICAR prior specifies each ϕ_i to be normally distributed with its mean equal to the mean of its neighbor's values. This is how the CAR/ICAR model "borrows strength" from geographic neighbors to smooth noisy estimates. Intuitively, the variance of each ϕ_i decreases as its number of neighbors d_i increases. The conditional distribution for each ϕ_i can be written

$$\text{p}(\phi_i \mid \phi_{i \sim j}) = \text{Normal}(\frac{\sum_{i \sim j} \phi_i}{d_i}, \frac{\sigma_i^2}{d_i})$$

Here, the variance σ is unknown. The conditional specification of each ϕ_i is helpful in building intuition about the assumptions the ICAR component makes and how it performs its "smoothing". The ICAR prior matches our intuition about spatial autocorrelation: areal unit i is similar to the areal units surrounding it,

and the more areal units surround it, the more confident we feel in that similarity. The joint distribution can be rewritten

$$\mathrm{p}(\phi) \propto \exp(-\frac{1}{2}\sum_{i\sim j}(\phi_i - \phi_j)^2)$$

This pairwise difference specification is more computationally efficient to fit in Stan (Morris et al, 2019).

4.5.3 Besag-York-Mollie (BYM)

The specific ICAR model used in this analysis is the Besag-York-Mollie (BYM) Poisson model. The BYM is a "classical" spatial Bayesian method (Riebler et al, 2016). It is generally used in disease mapping studies to model rare events (ie, disease occurrence) in small areal units. The BYM capitalizes on the ICAR prior's ability to smooth noisy estimates and share information across geographic units.

The latent function in the BYM model contains heterogeneous random effects as well as a spatial ICAR term in order to account for both spatial and non-spatial heterogeneity. Note that in Section _____, we introduced a random effect term θ. Therefore, the BYM model can be though of as decomposing θ into spatial and non-spatial components.

Specifically, the BYM model replaces η_i from equation _____ with

$$\eta_i = \beta_0 + \sum_{k=1}^{K} x_k^T \beta_k + \theta + \phi$$

where ϕ is the addition: an ICAR component. Decomposing overdispersion as such is helpful in furthering our understanding of response Y. When we use a simple random effect θ alone, we can accomplish a good model fit. However, θ provides no additional information about Y. The decomposition of θ in the BYM allows us to better quantify how much variance is white noise (ordinary random effects) versus some unmeasured confounding correlated across space.

The BYM model as written above is appealing in its simplicity. However, the lack of informative hyperpriors specified for θ and ϕ can make the model incredibly challenging to fit. In theory, extra-Poisson variance could be explained 100% by θ, 100% by ϕ, or anywhere in between. In *practice*, we likely have limited information about where that ratio falls. Riebler et al (2016) further explain the sampling issues faced by the BYM model faced with no hyperpriors. In short, the sampler is forced to explore all possible combinations of θ and ϕ, no matter how unlikely a particular combination my be. In the context of fitting models with Stan, this is likely to cause unnecessarily long computation times and perhaps to yield biased posterior estimates.

There are some suggestions in the literature for setting hyperpriors for θ and ϕ (Besag and Mollie, 1991; Clayton and Montomoli, 1995). The existing methods, however, tend to rely on the specific data at hand which makes the selection of hyperparameters unnecessarily time consuming.

4.5.4 BYM2

The BYM2 model proposed by Simpson et al and further described in Riebler et al (2016) aims to solve these sampling problems. The BYM2 takes a more "fully Bayesian" approach to hyperprior/hyperparameter selection. The primary difference between the BYM and BYM2 models is the addition of a mixing parameter, ρ. The BYM2 model rewrites the BYM as

$$\eta_i = \beta_0 + \sum_{k=1}^{K} x_k^T \beta_k + ((\sqrt{\frac{\rho}{s}})\theta^* + ((\sqrt{1-\rho})\phi^*)\sigma$$

where $\rho \in (0, 1)$ determines how much variance/overdispersion is caused by spatial versus non-spatial error terms. Like the popular Leroux CAR prior, proposed by Leroux et al (2009), the BYM2 scales both θ and ϕ by σ, the standard deviation of the combined error terms (Morris et al, 2019). In this parameterization, s is a scaling factor such that $\text{Var}(\theta_i) \approx \text{Var}(\phi_i) \approx 1$. The equal unit variance is necessary for σ to truly be the standard deviation of the error terms.

Setting priors is somewhat more straightforward for the BYM2. The ICAR component, ϕ^* remains unchanged. Riebler and Morris recommend the prior $\theta \sim \text{Normal}(0, n)$ where n is the number of connected graphs in the neighborhood graph. In many cases, such as modeling data for all counties in a state, $n = 1$. When $n > 1$, the variance is different in each subgraph which affects σ and s. It is possible to fit the model in this case, although computation time is much longer.

A relatively vague Normal(0, 1) prior is appropriate for σ. Riebler et al (2016) propose either a Beta(1/2, 1/2) or more specialized, complex prior for mixing parameter ρ. For this study, we use the simpler Beta(1/2, 1/2) prior.

4.5.5 Model 4

Model 4 uses all 18 covariates of interest, no horseshoe priors, and decomposes $\theta\sigma$ into a set of random effects plus a spatial ICAR component.

This model converges much more efficiently than Model 2 or Model 3 due to careful reparameterization of the BYM by Riebler et al (2016). Future work could likely improve the speed of fitting Models 2 and 3.

Model 4 was run on four chains for 10,000 iterations each. The parameter estimates for Model 4 are below. Note that `n_eff` is lower than for Model 1 but significantly higher than Model 2 or 3.

Parameter	Rhat	n_eff	mean	sd	2.5%	97.5%
beta0	1.001	4770	-1.880	0.028	-1.937	-1.825
sigma	1.003	520	2.698	0.372	1.993	3.451
rho	1.002	514	0.888	0.038	0.793	0.941
theta[5]	1.000	17797	-0.179	0.777	-1.688	1.336
beta[1]	1.000	4322	0.034	0.047	-0.056	0.127
beta[2]	1.001	3801	0.061	0.035	-0.009	0.131
beta[3]	1.000	4203	-0.003	0.039	-0.080	0.073
beta[4]	1.001	4330	-0.049	0.044	-0.134	0.037
beta[5]	1.000	4706	0.209	0.042	0.127	0.292
beta[6]	1.000	4919	0.065	0.038	-0.009	0.138
beta[7]	1.002	3929	0.029	0.038	-0.046	0.104
beta[8]	1.000	6278	0.145	0.032	0.083	0.207
beta[9]	1.000	4607	-0.088	0.031	-0.150	-0.026
beta[10]	1.000	6145	0.014	0.029	-0.043	0.070
beta[11]	1.000	6978	-0.022	0.031	-0.083	0.040
beta[12]	1.000	6125	-0.068	0.034	-0.136	-0.002
beta[13]	1.000	5875	0.094	0.033	0.029	0.158
beta[14]	1.000	4743	-0.089	0.035	-0.157	-0.019
beta[15]	1.001	2720	0.076	0.039	0.001	0.151
beta[16]	1.000	6053	-0.029	0.031	-0.091	0.031

Table 4: Stan output for Model 4.

Like Models 2 and 3, the BYM2 model performs well in the posterior predictive check (Figure ___).

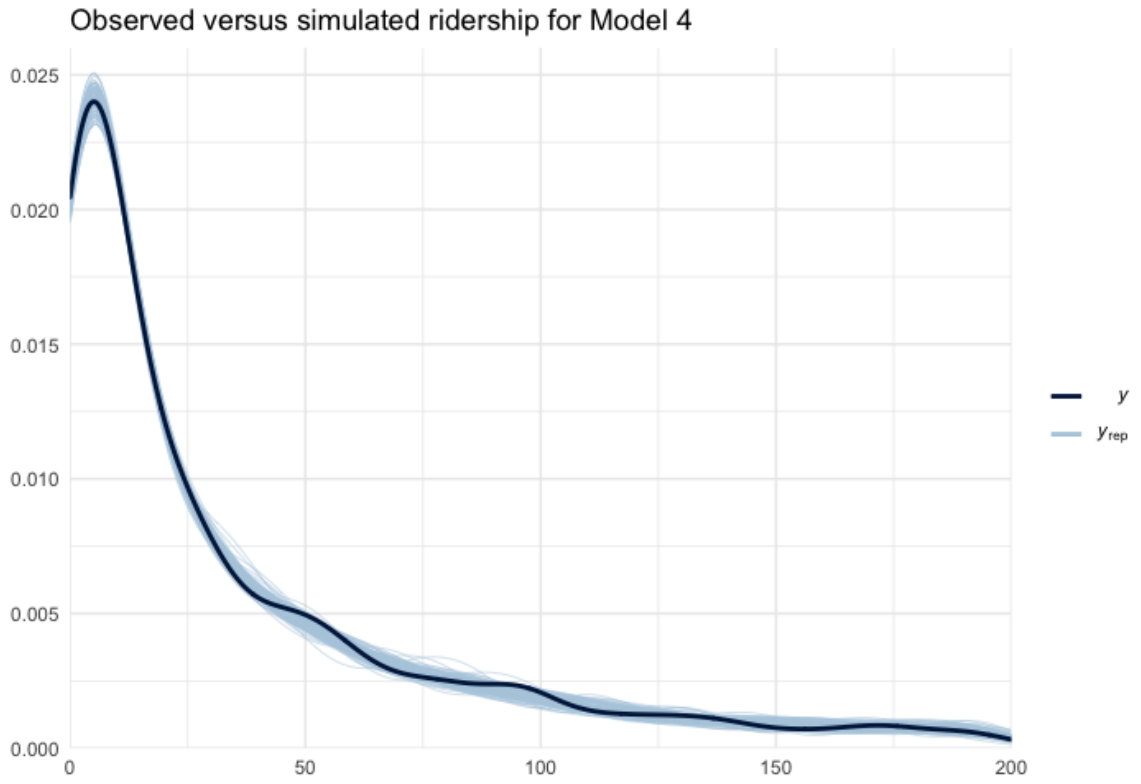

Figure 5: Posterior predictive check for Model 1.

4.5.6 Model 5

Model 5 builds upon Model 4 by incorporating regularized horseshoe priors in addition to spatial ICAR priors. This model has high autocorrelation between iterations and took *significantly* longer than any of the other models to fit in Stan (upwards of 12 hours). That said, the `n_eff` and $\hat{R}$ diagnostics indicate convergence and the parameter estimates (Table ___) match our expectations in terms of sign and magnitude based on the previous 4 models.

Parameter	Rhat	n_eff	mean	sd	2.5%	97.5%
beta0	1.000	5837	-1.878	0.028	-1.934	-1.822
sigma	1.010	721	2.826	0.359	2.138	3.561
theta[5]	1.000	19566	-0.188	0.787	-1.722	1.349
rho	1.012	713	0.900	0.031	0.824	0.946
phi[5]	1.004	1652	5.974	1.573	3.264	9.527
beta[1]	1.001	3637	-0.119	0.059	-0.233	-0.002
beta[2]	1.001	8170	-0.005	0.027	-0.069	0.049
beta[3]	1.000	3987	0.024	0.030	-0.019	0.096
beta[4]	1.000	8531	-0.004	0.022	-0.057	0.040
beta[5]	1.000	7619	-0.012	0.026	-0.076	0.030
beta[6]	1.001	2999	0.164	0.055	0.051	0.268
beta[7]	1.000	3726	0.032	0.035	-0.016	0.114
beta[8]	1.000	7956	0.010	0.025	-0.032	0.074
beta[9]	1.000	5622	0.019	0.028	-0.023	0.089
beta[10]	1.000	7530	0.144	0.033	0.079	0.208
beta[11]	1.000	4558	-0.057	0.034	-0.123	0.001
beta[12]	1.000	11150	0.004	0.018	-0.031	0.046
beta[13]	1.000	8289	-0.017	0.024	-0.073	0.020
beta[14]	1.000	5469	-0.028	0.031	-0.100	0.015
beta[15]	1.000	4822	0.060	0.035	-0.001	0.130
beta[16]	1.001	3863	-0.060	0.038	-0.134	0.003
beta[17]	1.000	2094	0.051	0.041	-0.008	0.137
beta[18]	1.000	6949	-0.010	0.021	-0.061	0.026

Table 5: Stan output for Model 5.

The posterior means for σ and ρ, as well as a "random" θ value are all similar to the posterior means of Model 4.

The posterior predictive checks and mapped residuals for Model 5 are very similar to those for Model 4. Like Model 2, the slow sampling time is largely caused by autocorrelation between iterations. In this case, the autocorrelation appears to be introduced by the horseshoe prior rather than by the well-parameterized BYM2.

The more interesting comparison here is with Model 3. The horseshoe priors in Model 5 fail to shrink any parameters *exactly* to zero. As previously discussed, running the model for more iterations would likely cause the coverage intervals on the β_k estimates to tighten.

5 Discussion/Results?

In this study, we fit several increasingly complex models building upon the baseline Poisson regression, Model 1. Model 2 incorporates a simple set of random effects to account for overdispersion. Model 3 incorporates regularized horseshoe priors for variable selection. Model 4 includes the spatial ICAR priors but no horseshoe priors, and Model 5 includes both regularized horseshoe priors and ICAR priors.

All five models were run for at least 10,000 iterations and "pass" the basic diagnostic checks: $\hat{R} = 1$, sufficiently high `n_eff`, and no concerning `max_treedepth` or divergence warnings.

Naturally, the baseline Model 1 converges most quickly and has the highest `n_eff` diagnostics. The simplicity of the Model, however, yields a poor model fit. Perhaps unexpectedly, Model 4, the BYM2, is the second-most efficient in terms of convergence and Effective Sample Size.

While the most complex model *does* converge and provide reasonable parameter estimates, its computational inefficiency may not be worth the addition of horseshoe priors to the BYM2 model, depending on the application. A more efficient approach may be to conduct variable selection using horseshoe priors on a simpler model (in our case, Model 1 or Model 3, for example) before incorporating the ICAR component.

The results of all five models fit in this study provide insights the existing Transit Market Areas cannot. Many of the results confirm institutional or intuitive knowledge at Metro Transit: for example, that "impermanence", represented here by percent of residents renting, is a good predictor of transit ridership.

once latex is working, this is where the table of posterior estimates was

5.1 Future Work

The work in this study will be the foundation of a temporal study at Metro Transit. In the process of fitting the models discussed above, Metro Transit data and covariates were prepared for years 2015-2018. Future work will include applying these models to each year and/or incorporating explicitly temporal trends into the models.

Many other covariates can be considered. The 18 selected for this study were selected largely based off of interest and perceived importance. Additional or more detailed demographic predictors could be incorporated: for example, percent of residents identified as immigrants (assuming recent immigrants may be transit reliant) or age or income breakdowns rather than simple medians. This study incorporated no land use characteristics or service-based predictors. Incorporating either could improve model fits or reveal new insights.

In a different vein, there is interest at Metro Transit in developing a "transit-specific geography" to solve the bounding problem discussed in Section ___ such that future models would not necessarily rely on geographic smoothing.

6 Appendix: Stan Code

6.1 Model 1

The Stan program for the baseline model is below. This model could also have been fit using Stan's more efficient built-in Poisson GLM function. For this study, we write the GLM more "longhand" for ease of comparison between models.

```
## data {
##   // number obs
##   int<lower=0> N;
##   // response
##   int<lower=0> y[N];
##   // "offset" (number of stops)
##   vector<lower=0>[N] E;
##   // number of covariates
##   int<lower=1> K;
##   // covariates
##   matrix[N, K] x;
## }
## transformed data {
##   vector[N] log_E = log(E);
## }
## parameters {
```

```
##   // intercept
##   real beta_0;
##   // covariates
##   vector[K] beta;
## }
## transformed parameters{
##   // latent function variables
##   vector[N] f;
##   f = log_E + beta_0 + x*beta;
## }
## model {
##   /// model
##   y ~ poisson_log(f);
##   // prior on betas
##   beta_0 ~ normal(0.0, 3);
##   beta ~ normal(0.0, 1);
## }
## generated quantities {
##   vector[N] log_lik;
##     for(i in 1:N) log_lik[i] = poisson_log_lpmf(y[i] | log_E[i] + beta_0 + x[i,]*beta);
## }
```

6.2 Model 2

The Stan program for Model 2 differs from Model 1 only in the latent variable, `f`.

```
## data {
##   // number obs
##   int<lower=0> N;
##   // response
##   int<lower=0> y[N];
##   // "offset" (number of stops)
##   vector<lower=0>[N] E;
##   // number of covariates
##   int<lower=1> K;
##   // covariates
##   matrix[N, K] x;
## }
## transformed data {
##   vector[N] log_E = log(E);
## }
## parameters {
##   // intercept
##   real beta_0;
##   // covariates
##   vector[K] beta;
##   // overdispersion
##   vector[N] theta;
##   // random effects variance
##   real<lower=0> sigma;
## }
## transformed parameters{
##   // latent function variables
```

```
##   vector[N] re;
##   vector[N] f;
##   re = theta * sigma;
##   f = log_E + beta_0 + x*beta + re;
## }
## model {
##   /// model
##   y ~ poisson_log(f);
##   // prior on betas
##   beta_0 ~ normal(0.0, 1);
##   beta ~ normal(0.0, 0.2);
##   // overdispersion
##   theta ~ normal(0, 1);
##   sigma ~ normal(0, 5);
## }
## generated quantities {
##   vector[N] log_lik;
##     for(i in 1:N) log_lik[i] = poisson_log_lpmf(y[i] | log_E[i] + beta_0 + x[i,]*beta + re[i]);
## }
```

6.3 Model 3

The regularized horseshoe prior used to fit Model 3 is adopted from Piironen and Vehtari.

```
## data {
##   // number obs
##   int<lower=0> N;
##   // response
##   int<lower=0> y[N];
##   // "offset" (number of stops)
##   vector<lower=0>[N] E;
##   // number of covariates
##   int<lower=1> K;
##   // covariates
##   matrix[N, K] x;
##   // prior sd for intercept
##   real<lower=0> scale_icept;
##   // scale for half t for tau
##   real<lower=0> scale_global;
##   // df for tau, lambda
##   real<lower=1> nu_global;
##   real<lower=1> nu_local;
##   // slab scale, df for reg horseshoe
##   real<lower=0> slab_scale;
##   real<lower=0> slab_df;
## }
## transformed data {
##   vector[N] log_E = log(E);
## }
## parameters {
##   // intercept
##   real beta_0;
##   // parameterization from vehtari
```

```
##   vector[K] z;
##   real<lower=0> aux1_global;
##   real<lower=0> aux2_global;
##   vector<lower=0>[K] aux1_local;
##   vector<lower=0>[K] aux2_local;
##   real<lower=0> caux;
## }
## transformed parameters {
##   // global shrinkage
##   real<lower=0> tau;
##   // local shrinkage
##   vector<lower=0>[K] lambda;
##   vector<lower=0>[K] lambda_tilde;
##   // slab scale
##   real<lower=0> c;
##   // regression coefficients
##   vector[K] beta;
##   // latent function variables
##   vector[N] f;
##
##   lambda = aux1_local .* sqrt(aux2_local);
##   tau = aux1_global * sqrt(aux2_global) * scale_global;
##   c = slab_scale * sqrt(caux);
##   lambda_tilde = sqrt(c^2 * square(lambda) ./ (c^2 + tau^2 * square(lambda)));
##   beta = z .* lambda_tilde*tau;
##   f = log_E + beta_0 + x*beta;
## }
## model {
##   // half t and inverse gamma priors
##   z ~ normal(0, 1);
##   aux1_local ~ normal(0, 1);
##   aux2_local ~ inv_gamma(0.5*nu_local, 0.5*nu_local);
##   aux1_global ~ normal(0, 1);
##   aux2_global ~ inv_gamma(0.5*nu_global, 0.5*nu_global);
##   caux ~ inv_gamma(0.5*slab_df, 0.5*slab_df);
##   beta_0 ~ normal(0, scale_icept);
##   // and the model
##   y ~ poisson_log(f);
## }
## generated quantities {
##   vector[N] log_lik;
##     for(i in 1:N) log_lik[i] = poisson_log_lpmf(y[i] | log_E[i] + beta_0 + x[i,]*beta);
## }
```

6.4 Model 4

The BYM2 model is fit using code from Morris et al.

```
## data {
##   int<lower=0> N;
##   int<lower=0> N_edges;
##   int<lower=1, upper=N> node1[N_edges];  // node1[i] adjacent to node2[i]
##   int<lower=1, upper=N> node2[N_edges];  // and node1[i] < node2[i]
```

```
##
##   int<lower=0> y[N];              // count outcomes
##   vector<lower=0>[N] E;           // exposure
##   int<lower=1> K;                 // num covariates
##   matrix[N, K] x;                 // design matrix
##
##   real<lower=0> scaling_factor; // scales the variance of the spatial effects
## }
## transformed data {
##   vector[N] log_E = log(E);
## }
## parameters {
##   real beta0;            // intercept
##   vector[K] beta;       // covariates
##
##   real<lower=0> sigma;        // overall standard deviation
##   real<lower=0, upper=1> rho; // proportion unstructured vs. spatially structured variance
##
##   vector[N] theta;       // heterogeneous effects
##   vector[N] phi;         // spatial effects
## }
## transformed parameters {
##   vector[N] convolved_re;
##   vector[N] f;
##   // variance of each component should be approximately equal to 1
##   convolved_re =  sqrt(1 - rho) * theta + sqrt(rho / scaling_factor) * phi;
##
##   f = log_E + beta0 + x * beta + convolved_re * sigma;
## }
## model {
##   y ~ poisson_log(f);  // co-variates
##
##   // This is the prior for phi! (up to proportionality)
##   target += -0.5 * dot_self(phi[node1] - phi[node2]);
##
##   beta0 ~ normal(0.0, 1.0);
##   beta ~ normal(0.0, 1.0);
##   theta ~ normal(0.0, 1.0);
##   sigma ~ normal(0, 1.0);
##   rho ~ beta(0.5, 0.5);
##   // soft sum-to-zero constraint on phi)
##   sum(phi) ~ normal(0, 0.001 * N);  // equivalent to mean(phi) ~ normal(0,0.001)
## }
## generated quantities {
##   vector[N] log_lik;
##     for(i in 1:N) log_lik[i] = poisson_log_lpmf(y[i] | log_E[i] + beta0 + x[i, ] * beta + convolved_
## }
```

6.5 Model 5

Finally, the code to fit Model 5 quite literally combines the programs for Models 3 and 4.

```
## data {
```

```
##   int<lower=0> N;
##   int<lower=0> N_edges;
##   int<lower=1, upper=N> node1[N_edges];  // node1[i] adjacent to node2[i]
##   int<lower=1, upper=N> node2[N_edges];  // and node1[i] < node2[i]
##
##   int<lower=0> y[N];              // count outcomes
##   vector<lower=0>[N] E;           // exposure
##   int<lower=1> K;                 // num covariates
##   matrix[N, K] x;                 // design matrix
##
##   real<lower=0> scaling_factor; // scales the variance of the spatial effects
##
##   //horseshoe
##   // prior sd for intercept
##   real<lower=0> scale_icept;
##   // scale for half t for tau
##   real<lower=0> scale_global;
##   // df for tau, lambda
##   real<lower=1> nu_global;
##   real<lower=1> nu_local;
##   // slab scale, df for reg horseshoe
##   real<lower=0> slab_scale;
##   real<lower=0> slab_df;
## }
## transformed data {
##   vector[N] log_E = log(E);
## }
## parameters {
##   real beta0;            // intercept
##
##   real<lower=0> sigma;        // overall standard deviation
##   real<lower=0, upper=1> rho; // proportion unstructured vs. spatially structured variance
##
##   vector[N] theta;       // heterogeneous effects
##   vector[N] phi;         // spatial effects
##
##   // horseshoe
##   vector[K] z;
##   real<lower=0> aux1_global;
##   real<lower=0> aux2_global;
##   vector<lower=0>[K] aux1_local;
##   vector<lower=0>[K] aux2_local;
##   real<lower=0> caux;
## }
## transformed parameters {
##   vector[N] convolved_re;
##
##   // horseshoe
##     // global shrinkage
##   real<lower=0> tau;
##   // local shrinkage
##   vector<lower=0>[K] lambda;
##   vector<lower=0>[K] lambda_tilde;
##   // slab scale
```

```
##   real<lower=0> c;
##   // regression coefficients
##   vector[K] beta;
##   // latent function variables
##   vector[N] f;
##
##   lambda = aux1_local .* sqrt(aux2_local);
##   tau = aux1_global * sqrt(aux2_global) * scale_global;
##   c = slab_scale * sqrt(caux);
##   lambda_tilde = sqrt(c^2 * square(lambda) ./ (c^2 + tau^2 * square(lambda)));
##   beta = z .* lambda_tilde*tau;
##
##   // variance of each component should be approximately equal to 1
##   convolved_re =  sqrt(1 - rho) * theta + sqrt(rho / scaling_factor) * phi;
##
##   f = log_E + beta0 + x * beta + convolved_re * sigma;
## }
## model {
##   y ~ poisson_log(f);  // co-variates
##
##   // This is the prior for phi! (up to proportionality)
##   target += -0.5 * dot_self(phi[node1] - phi[node2]);
##
##   beta0 ~ normal(0.0, scale_icept);
##   theta ~ normal(0.0, 1.0);
##   sigma ~ normal(0, 1.0);
##   rho ~ beta(0.5, 0.5);
##   // soft sum-to-zero constraint on phi)
##   sum(phi) ~ normal(0, 0.001 * N);  // equivalent to mean(phi) ~ normal(0,0.001)
##
##   //horseshoe
##     // half t and inverse gamma priors
##   z ~ normal(0, 1);
##   aux1_local ~ normal(0, 1);
##   aux2_local ~ inv_gamma(0.5*nu_local, 0.5*nu_local);
##   aux1_global ~ normal(0, 1);
##   aux2_global ~ inv_gamma(0.5*nu_global, 0.5*nu_global);
##   caux ~ inv_gamma(0.5*slab_df, 0.5*slab_df);
##   beta0 ~ normal(0, scale_icept);
## }
## generated quantities {
##   vector[N] log_lik;
##     for(i in 1:N) log_lik[i] = poisson_log_lpmf(y[i] | log_E[i] + beta0 + x[i, ] * beta + convolved_
## }
```